

RESEARCH ARTICLE

Distinct tropical Pacific sea surface temperature anomaly regimes enhanced under recent global warming

Jing Li¹  | Lin Mu^{2,3} | Linhao Zhong⁴ 

¹College of Marine Science and Technology, China University of Geosciences, Wuhan, China

²College of Life Sciences and Oceanography, Shenzhen University, Shenzhen, China

³Shenzhen Research Institute, China University of Geosciences, Shenzhen, China

⁴Key Laboratory of Regional Climate-Environment for Temperate East Asia, Institute of Atmospheric Physics, Chinese Academy of Sciences, Beijing, China

Correspondence

Lin Mu, College of Life Sciences and Oceanography, Shenzhen University, Shenzhen 518060, China.
Email: mulin@szu.edu.cn

Linhao Zhong, Institute of Atmospheric Physics, Chinese Academy of Sciences, Beijing 100029, China.
Email: zlh@mail.iap.ac.cn

Funding information

Key-Area Research and Development Program of Guangdong Province, Grant/Award Number: 2020B1111020005; Discipline Layout Project for Basic Research of Shenzhen Science and Technology Innovation Committee, Grant/Award Number: JCYJ20170810103011913

Abstract

El Niño and Southern Oscillation (ENSO) events are usually monitored by tropical Pacific sea surface temperature anomaly (SSTA) patterns with dramatic impacts on the global climate. To explore the diversity of the tropical Pacific SSTA, a novel method combined empirical orthogonal function analysis and the K-means clustering algorithm is carried out to classify SSTA patterns during 1950–2016. Meanwhile, the total distance variance and total silhouette value are introduced to determine an optimal number of distinguishable representative SSTA patterns. Ten SSTA patterns are obtained, which shows frequent basin-wide warming and extreme cold ENSO events in recent decades. It may be attributed to the changes in composition of the intrinsic modes along with the background mode of slowly increasing east–west SST gradient. The comparative analysis between periods 1950–1969 and 1997–2016 suggests that the two regimes of tropical Pacific SSTA, featured as extreme warm and moderate warm/extreme cold patterns respectively, become more distinct under recent global warming.

KEYWORDS

clustering, K-means, sea surface temperature anomalies (SSTA) diversity

1 | INTRODUCTION

El Niño and Southern Oscillation (ENSO) is the dominant interannual mode of sea surface temperature anomalies (SSTA) in the equatorial eastern Pacific (EP). However, an unusual mode of ENSO with maximum warming in the central equatorial Pacific during the summer of 2004 was observed and named by El Niño Modoki (Ashok *et al.*, 2012). Since then, a number of studies have conducted

to identify, describe, and understand the different spatial patterns of SSTA, especially for the central Pacific (CP) and the EP El Niño (e.g., Leloup *et al.*, 2007; Takahashi *et al.*, 2011; Johnson, 2013; Capotondi *et al.*, 2015).

With the accumulated CP El Niño events, it has been regarded as a possible harbinger of changes in tropical Pacific SSTA patterns under global warming (Yeh *et al.*, 2009). Yeh *et al.* (2009) reported that the increasing ratio of CP- to EP-type El Niño can be observed in both

CMIP3 and CMIP5 simulations under global warming scenarios. However, a great uncertainty still exists in their recent study (Power *et al.*, 2013; Yeh *et al.*, 2014). Generally, the tropical Pacific SSTA spatial patterns of ENSO are neither only EP nor CP types, but rather many different flavours (Capotondi *et al.*, 2015). Besides the CP warming events, large basin-wide warming events are also expected to occur under global warming (Ashok *et al.*, 2012). In addition, extreme cold and warm ENSO events with CP cooling centre and EP warming centre respectively are also predicted to increase in frequency under global warming (Cai *et al.*, 2014, 2015a). Although many studies have been devoted to the SSTA patterns, especially the ENSO flavours. The impact of global warming on the tropical Pacific SSTA patterns is still difficult to evaluate. For instance, the SSTA spatial patterns could be intrinsically modulated even if there is no external forcing (Zebiak and Cane, 1987; Wittenberg, 2009). Furthermore, as various datasets show different signs of their trend in the EP and CP, the sea surface anomaly trends in the equatorial Pacific are particularly controversial (L'Heureux *et al.*, 2013).

Hence, two questions arise: How many flavours of the tropical Pacific SSTA pattern can be objectively derived? Is there any change in the SSTA flavours under recent global warming?

To address the two questions, a novel method which combines the empirical orthogonal function (EOF) analysis and K-means clustering algorithm is applied to classify the SSTA spatial patterns objectively. This method allows us to connect the changes in SSTA spatial patterns to the tropical Pacific modes. The remainder of the paper is organized as follows. Section 2 provides the descriptions of the datasets and the methods. The dominant modes are illustrated in Section 3. The SSTA flavours and their changes are shown in Section 4. The regime changes as well as the possible reasons are discussed in Section 5. Finally, conclusions and discussions are highlighted.

2 | DATA AND METHODS

We firstly examined the monthly Met Office Hadley Sea Ice and SST dataset (HadISST1; Rayner *et al.*, 2003). Then the Centennial Observation-Based Estimates (COBE) of SST (Ishii *et al.*, 2005) and Extended Reconstructed Sea Surface Temperature (ERSST) v4 (Huang *et al.*, 2015) were also supplemental to confirm our results. The global surface air temperature anomalies were obtained from the third Met Office Hadley Centre and Climatic Research Unit Global Land and Sea Surface Temperature Data Set (HadCRUT3) (Brohan *et al.*, 2006).

With the widespread attention on the different SSTA flavours, some cluster methods have been proposed to identify the ENSO and related convection flavours. Among these related studies, EOF seems to be the most popular method. However, because of its orthogonality constraint, EOF analysis has a tendency to produce unphysical modes. To overcome the limitation of EOF, some clustering methods are also introduced. For example, Johnson (2013) introduced a self-organizing map (SOM) classification method with a statistical distinguishability test based on the September–February mean SST data during 1950–2011 to identify the tropical Pacific SST anomaly patterns. Su *et al.* (2018) obtained 13 clusters by applying K-means clustering to equatorial Pacific averaged SSTA. Despite the limitations of EOF, EOF is still a widely used and powerful downscaling method for tropical SSTA issues. The physical interpretation of the leading modes of the tropical Pacific SSTA are also deeply analysed and widely accepted. Therefore, there are also some studies by the combinations of EOF modes. Takahashi *et al.* (2011) pointed that the complexity of the tropical Pacific SSTA can be depicted by two EOF modes into two regimes: extreme warm events and ordinary cold and moderately warm events. Ding *et al.* (2018) performed the EOF analysis on the OLR dataset and distinguished different patterns by combining the first two EOFs with their phases.

Inspired by their studies, a novel method is proposed combining the EOF method and the K-means clustering method. An EOF analysis was carried out to decompose the dominant modes of the tropical Pacific SST anomaly over the region of 30°S–30°N, 110°E–70°W for downscaling. The three leading EOFs with the particular characteristics of special SSTA patterns which has been widely studied by many previous researchers are selected for following clustering. Considering the previous studies on the three leading modes, it does favour on understanding the cluster results. Then to overcome the disadvantages of EOF analysis in capturing the SSTA patterns (Leloup *et al.*, 2007), the K-means clustering method (Jiang *et al.*, 2016; https://ww2.mathworks.cn/help/stats/kmeans.html?s_tid=doc_ta) was applied on the corresponding principal components (PCs) of the three leading EOF modes of SSTA. K-means clustering method is a no class label and unsupervised learning technique. It is a group partitioning method which can reduce the high-dimensional data space (in this study, three PCs over 804 months). In addition, the total distance variance (TDV) (Jiang *et al.*, 2016) and total silhouette value (Kaufman and Rousseuw, 1990) were introduced to specify the optimal number of groups beforehand. In addition, composite and correlation analyses were also carried out.

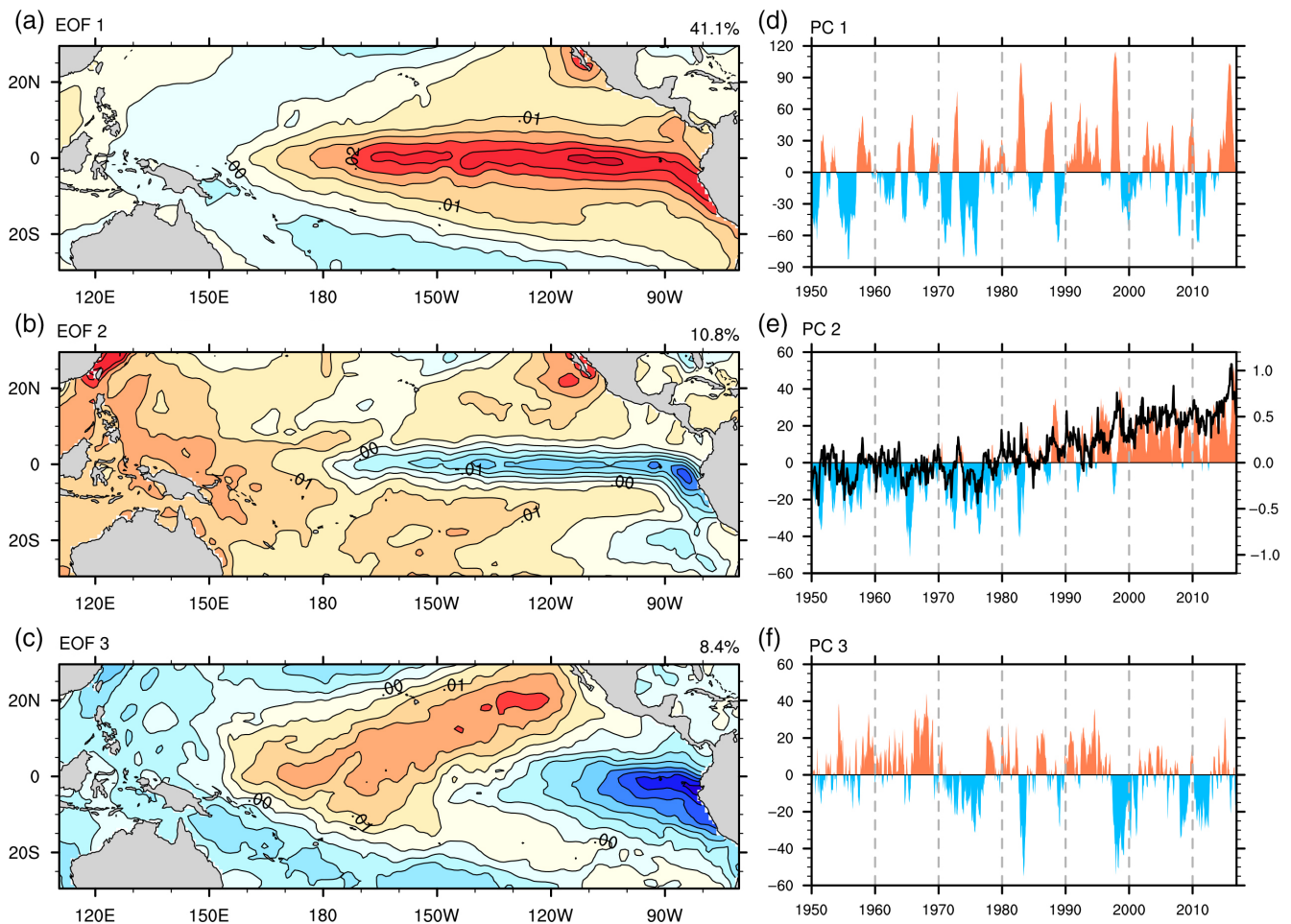


FIGURE 1 The EOF analysis of tropical Pacific SSTA variability during 1950–2016. The three EOF leading modes (a–c) and their corresponding PCs (d–f; scale on the left axis). The time series of monthly mean global air temperature anomaly is plotted in e (black line; scale on right axis)

3 | DOMINANT MODES OF SSTA IN THE TROPICAL PACIFIC

Figure 1 shows the three EOF normalized leading modes of SSTA and the time series of PC based on the HadISST1 dataset during 1950–2016. These modes of SSTA are robust and confirmed by other datasets (Takahashi *et al.*, 2011; L'Heureux *et al.*, 2013). The EOF1 and EOF3 are particularly stable, and do not change with the selections of datasets and time periods, and they can also be accurately reproduced by the CMIP5 models (Xu *et al.*, 2017). The first EOF mode clearly resembles the canonical El Niño pattern, which accounts for 41.1% of total variance of SSTA. The third EOF mode is similar as the El Niño Modoki, which explains 8.4%. Ashok *et al.* (2007) uncovered this mode as the second EOF using HadISST during 1979–2004. However, Hoerling *et al.* (1997) reported that this pattern is also prone to reveal the character of spatial asymmetry between the EP El Niño and La Niña Patterns, so it reminds us of the Pacific

meridional mode (PMM) (L'Heureux *et al.*, 2013). Research suggests this particular SSTA mode is not uniquely identified in CP ENSO events (Johnson, 2013), but a ‘modulator’ for reflecting inter-event differences which seldom appears without a substantial projection onto EOF1 (Cai *et al.*, 2015b). Most of the ENSO flavours can be generally duplicated by the combinations of EOF1 and EOF3 modes of SSTA (Capotondi *et al.*, 2015; Cai *et al.*, 2015b). In this regard, these two EOF patterns are defined as the intrinsic modes of SSTA in this study.

EOF2 shares some characteristics with EOF1, representing an out-of-phase relationship of SST anomaly variability between the Pacific cold tongue region and else in the tropical Pacific, but its existence strongly depends on the linear trends of SST over the tropical Pacific Ocean (L'Heureux *et al.*, 2013). The corresponding PC2 is highly correlated with global mean surface temperature (Figure 1e). This mode, also referred as the ‘cooling mode’, has been attributed to global warming (Zhang *et al.*, 2010), and it possibly reflects the dynamic

effect, such as increasing upwelling, in the eastern equatorial Pacific Ocean (Cane *et al.*, 1997). L'Heureux *et al.* (2013) pointed out that this mode merely depends on the linear trends over the tropical Pacific Ocean. The 'cooling mode' still exists even when the EOF is applied to a shorter-record of SSTA (1979–2010), where it resembles the third leading mode, captured by a slowly intensifying background in the zonal gradient of SSTA (Ashok *et al.*, 2012). Hence, the second EOF mode acts as a background mode of SSTA.

The three leading EOF modes explain about 60% of the total variance of SSTA variability in the tropical Pacific and reflect the diversity of SSTA patterns. The robustness of these modes can be confirmed by different datasets and supported by other works. For instance, Takahashi *et al.* (2011) reinterpreted these intrinsic modes of the canonical and Modoki El Niño and attributed them to the nonlinear evolution of SSTA diversity. Based on the linear combinations of EOF1 and EOF2 (background mode), Ashok *et al.* (2012) hypothesized that more basin-wide warm SSTA events possibly due to further global warming.

4 | CHANGES IN THE DIVERSITY OF TROPICAL PACIFIC SSTA PATTERNS

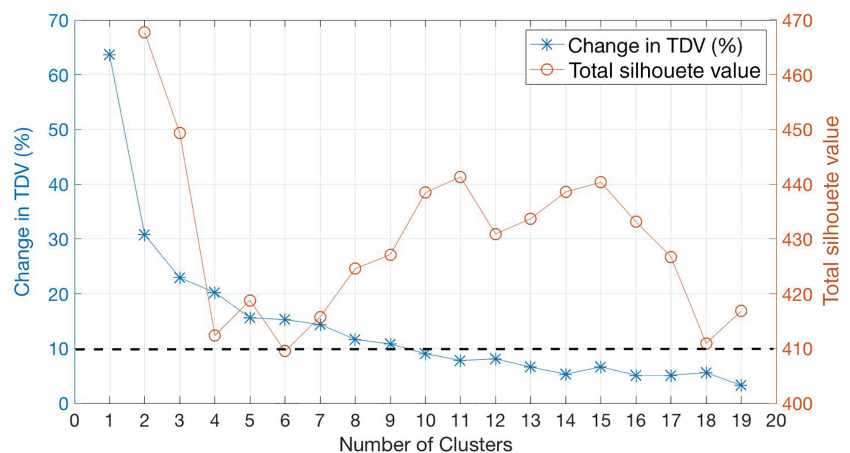
The three leading modes can explain most of SSTA variability over the tropical Pacific, and then the SSTA of all the months (samples) are characterized by the three corresponding PCs. Here we apply the K-means clustering algorithm using cosine distance measures to the three PCs, and aim to identify the common performance of SSTA patterns over the last 67 years. In this study, TDV and total silhouette value were used to determine a reasonable cluster number (Figure 2). The change of TDV denotes the difference between cluster number of K and

K + 1. The smaller change, the more stable clustering results. And the total silhouette value represents the separation distance between the resulting clusters. It helps to evaluate the correctness of the allocation of the data sample in the specified cluster instead of another cluster by measuring both inter-cluster separation and intra-cluster cohesion (Ogbuabor and Ugwoke, 2018). That is, determinate the maximum number of SSTA patterns requires maximize similarity within groups while maximizing distinction between groups. According to the principle, 10% TDV change is recommended to set (Jiang *et al.*, 2016), and the SSTA fields of all the months are reasonably clustered into 10 clusters. The PC-based combinations of the 10 cluster centroids and their related SSTA cluster patterns by the sample composition are presented in Figure 3.

The different combination of leading three PCs produces various SSTA patterns. Figure 3b–k shows the SSTA spatial differentiation associated with 10 clusters. Three La Niña-like SSTA patterns (cluster 4, cluster 6 and cluster 7) and three El Niño-like patterns (cluster 2, cluster 5 and cluster 9) are contained. Cluster 9 resembles the so-called canonical EP El Niño, and its opposite phase seems like cluster 6 repressing the extreme La Niña with a cooling centre near the CP. Cluster 4 shows a basin-wide cooling spatial pattern, and cluster 2 resembles the basin-wide warming events (Ashok *et al.*, 2012) also with a CP centre. Cluster 5 expresses a typical CP El Niño pattern. Cluster 10 seemingly represents the PMM. And cluster 8 denotes the called 'cooling mode' (Zhang *et al.*, 2010).

In order to depict the change of tropical Pacific SSTA patterns diversity clearly, the 10 cluster patterns are further grouped into warm (red boxes) and cold (blue boxes) groups according to the mean Nino 3.4 indices of their members (Figure 4a). The cumulative frequency (months) of each cluster pattern is shown in Figure 4b, where the slopes show the frequencies for each cluster

FIGURE 2 Change in TDV (blue; scale on the left axis) and the total silhouette value (red; scale on the right axis) versus the number of clusters. Based on previous work, 10% TDV change is suggested to set as an objective criterion for determining the optimal number of clusters, while the total silhouette value cannot be very small. Finally, 10 clusters are determined for this study. Details are referred to the reference cited in the paper



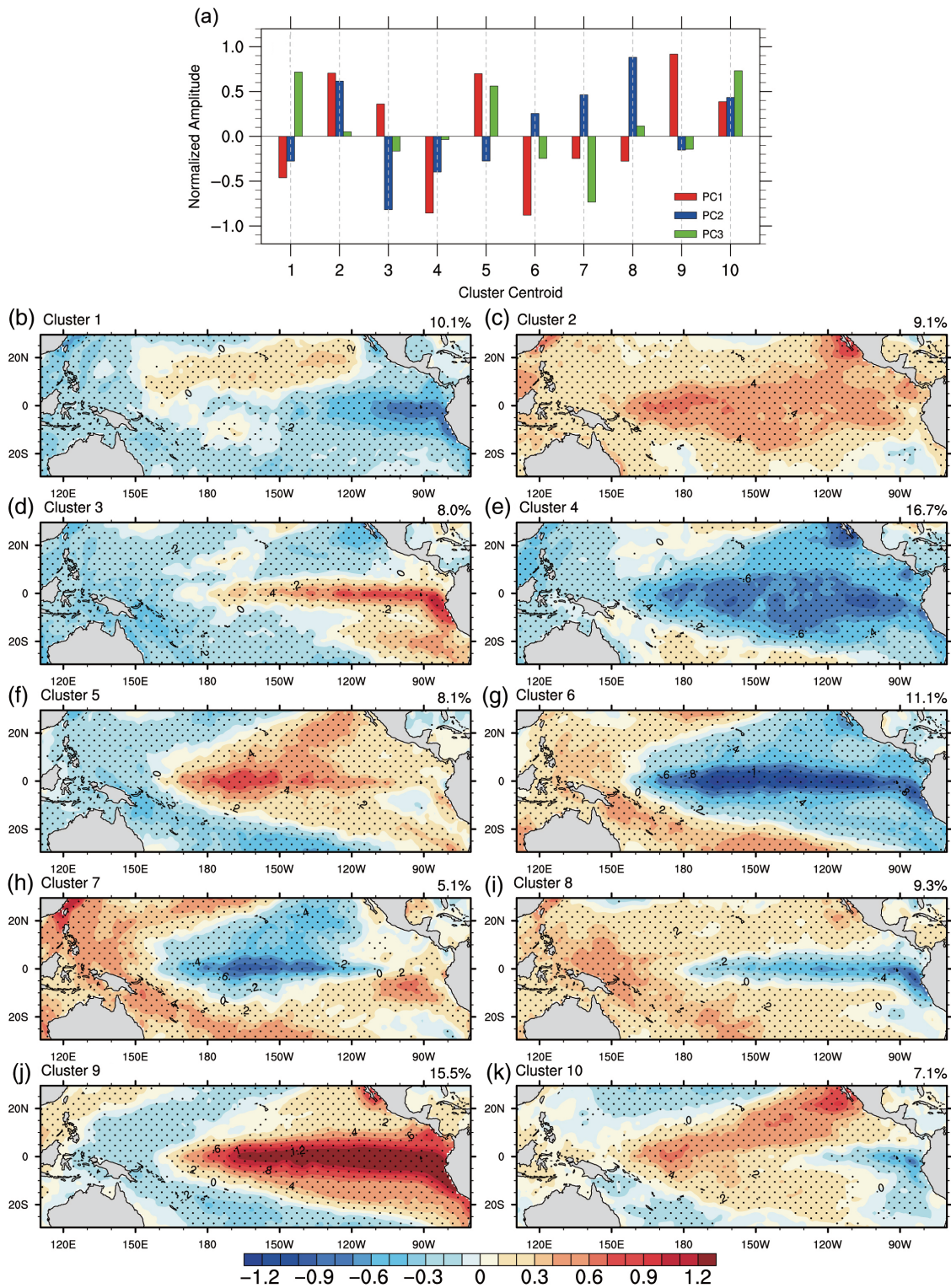


FIGURE 3 (a) Normalized amplitudes of three PCs for each centroid of 10 clusters. (b–k) The spatial patterns of 10 clusters in SST anomalies ($^{\circ}\text{C}$), where the dots indicate the area exceeding 95% significance based on a t -test

pattern. The cumulative frequency in Figure 4b shows that warm cluster patterns (3, 5 and 9) and cold cluster patterns (1 and 4), the dominant modes before 1980s, have quasi-periodicity feature. Since the middle 1980s,

cluster patterns 1, 3, 4 and 5 have never occurred again, which can be identified by their horizontal cumulative frequency lines in recent decades in Figure 4b. Cluster pattern 9 occurs steadily before it reaches the inflection

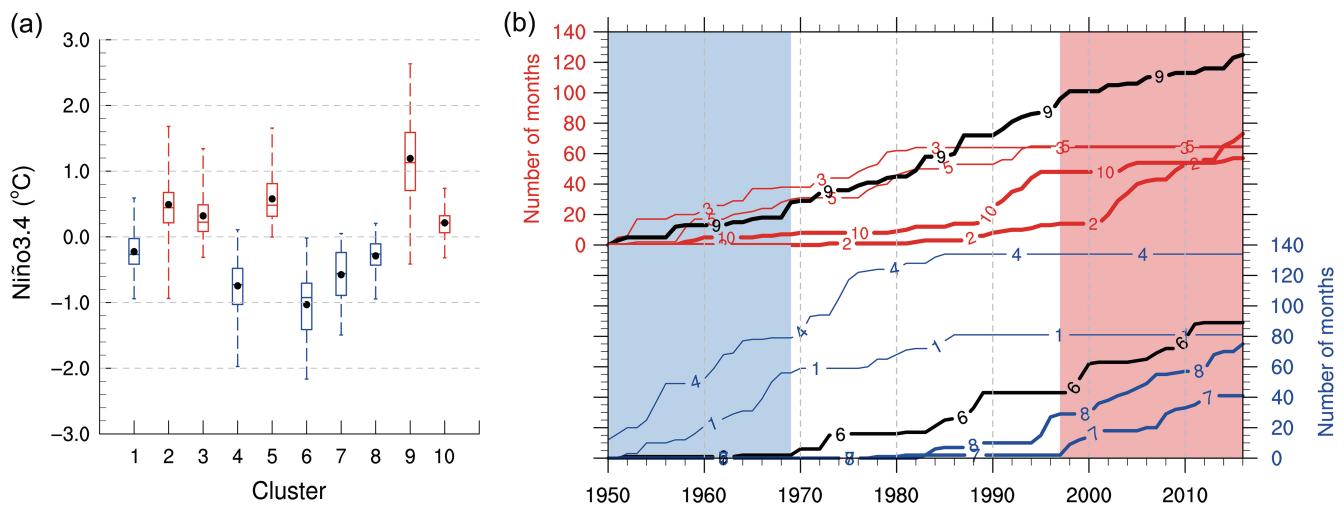


FIGURE 4 (a) Box plots of the Niño 3.4 SSTA index for each of 10 clusters with whiskers from minimum to maximum. The box plots represent the Niño 3.4 SSTA index distributions of the members in their corresponding clusters. The bottom, median and top lines in each box are the first, second and third quartiles of Niño 3.4 SSTA index, and the black dots indicate their averages. (b) The time series of the cumulative numbers (months) from each of 10 clusters, which is marked by the cluster numbers in Figure 3. The early and recent two decades of 1950–1969 and 1997–2016 are shaded by blue and red bars, respectively

point in the late 1990s, when it exhibits a lower frequency.

Similarly, the cold cluster pattern 6 with respect to the extreme La Niña shows a quasi-periodicity feature since the early 1970s before the cluster pattern 1 displays a lower frequency, which indicates westward of their cooling centres. Cluster patterns 7 and 8 start to be active since the middle 1990s, which resembles the CP La Niña and the ‘cooling mode’ of SSTA, respectively. Among the 10 clusters, the most significantly increasing frequency is found in cluster 2, resembling a basin-wide warming pattern, as a result of the combination of PC1 and PC2 with the same sign. This result is consistent to the implication of Ashok *et al.* (2012) who indicated that the basin-wide warm events are expected to be increasing under any further global warming.

Among the 10 cluster patterns some usually fail to meet the standards of ‘ENSO events’, such as clusters 1, 3, 8 and 10 (Figure 4a). In addition to the canonical ENSO patterns (clusters 9), extreme La Niña events (cluster 6), basin-wide warming events (cluster 2) and CP La Niña (cluster 7) events occurred more frequently in recent decades. The dramatic changes in the tropical Pacific SSTA seem to occur around the 1980s. As ENSO events usually peak in winter (December–January–February), the changes of SSTA diversity in winter imply the changes of the ENSO events. Similarly, as shown in Figure 5, it seems that the basin-wide cooling ENSO events (cluster 4) occurred most frequently for the first 20 years (1950–1969), and clusters 2, 6, 7, 8, 10 never occurred in that time. While during the last

20 years (1997–2016), except for the canonical EP El Niño events (cluster 9), the frequent clusters in the first 20 years never appeared. And the extreme La Niña events (cluster 6) display a high frequency in recent decades. In general, considering these frequent patterns, it seems that the SSTA centres for both the warm and cold ENSO events seem to move westward since the 1980s.

5 | TROPICAL PACIFIC SSTA REGIMES UNDER RECENT GLOBAL WARMING

Fedorov and Philander (2000) suggested that global warming may alter the background of SST anomaly and then affect ENSO diversity. Though the linear trends of SSTA and global warming are controversial, the high correlation between the background mode (‘cooling mode’) and global warming is evident. Therefore, the linkage of SSTA diversity with background mode is discussed.

The 10 modes are clustered to depict the change of SSTA patterns diversity, which is mainly determined by the combinations of the three leading modes. It seems that the changes in the tropical Pacific SSTA diversity are close related to the background mode of EOF2, whose phase transition from negative to positive also takes place around the 1980s. However, except for the basin-wide warming events (cluster 2), most of the frequent SSTA patterns after the 1980s cannot be simply interpreted by the linear superposition of the ‘cooling mode’ (EOF2).

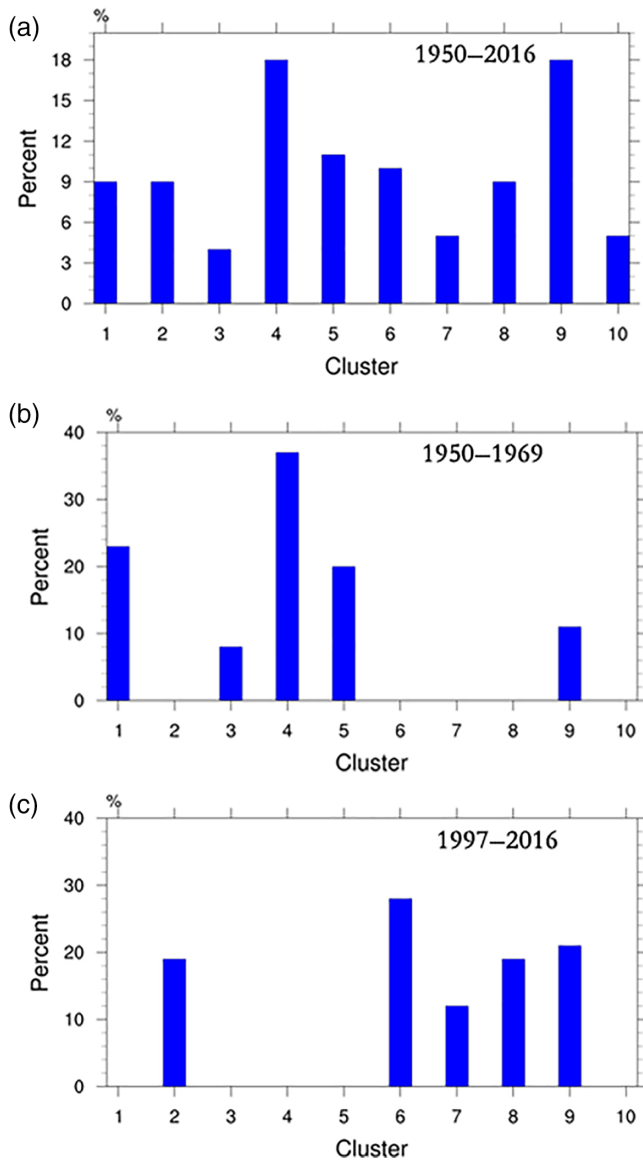


FIGURE 5 The percentage of occurrence frequency (months) of 10 clusters respectively in winter (December–January–February) during (a) 1950–2016, (b) 1950–1969, (c) 1997–2016

Though EOF2, characterized by a slowly intensifying west–east gradient of SSTA, acts as a background mode, the change of PC2 from negative to positive phases also implies an alteration from cluster patterns 3–8. These two patterns usually act as the initial states of the ENSO events and induce the change of the anomalous westerly and easterly respectively. A recent study suggested that the response of zonal winds to the warm SSTA is greater than that to the cold SSTA in the central to east tropical Pacific, which can be considered as the source of ENSO asymmetry (Cai *et al.*, 2015b).

To explore the possible reasons behind the change of SSTA diversity under global warming, periods 1950–1969

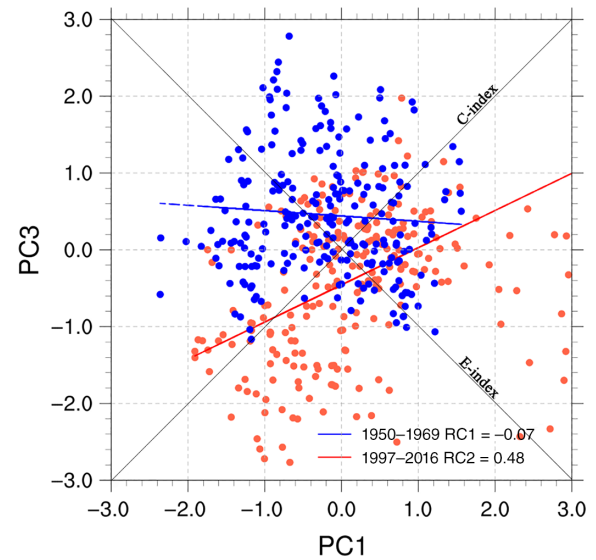


FIGURE 6 Scatter plot of normalized PC1 (x-axis) against PC3 (y-axis) of each sample during 1950–1969 (blue dots) and 1997–2016 (red dots) with linear regression lines

and 1997–2016 (the first and last 20 years) with negative and positive PC2 phases are respectively selected. In previous study, Takahashi *et al.* (2011) defined two indices, the $(PC1 - PC3)/\sqrt{2}$ as E index and the $(PC1 + PC3)/\sqrt{2}$ as C index, and applied them to evaluate the value of intrinsic modes of SSTA. The C index accounts for the cold, neutral, and moderate warm events of SSTA while the E index quantifies the departure from the C index. The latter is usually relative to extreme warm ENSO events. Then the regime changes along with the phase transition of the ‘cooling mode’ are discussed. The samples during these two periods are displayed in the scatter plot (Figure 6). In this regard, cluster patterns 5, 6, 7 and 10 whose PC1 and PC3 are in phase (both positive or negative; Figure 3a) are close to C index, and most of them appeared after 1980s (as shown in Figure 4b). Furthermore, the linear regression lines of 1997–2016 (red line in Figure 6) implies that a significant positive correlation is found between PC1 and PC3 during this time, except of some extreme ENSO events. During 1950–1969, however, the linear regression lines almost parallels to PC1 axis, which indicates the relationship between PC1 and PC3 seems chaotic. A clear shift is found from the early to the recent decades in C indices (Figure 6, Figure S1 and Figure S2 for other datasets as well as different periods). And in recent period, more extreme warm ENSO events away from the C index are also observed despite the limited extreme warm ENSO cases. Considering the E index is mainly used to quantify the departure from the C index (Takahashi *et al.*, 2011), the regimes of C-index and E-

index are speculated to be more distinct along with the phase transition of the 'cooling mode'.

In contrast to the early stage, samples (red dots) generally have large negative values in the C index, bringing about the maximum cooling SSTA in the CP (Figure 6), such as cluster patterns of 6 and 7. For the E index, the blue and red dots depart from the C index in an opposite direction. Most blue dots away from the C index are located in the negative E index phase, resembling a weak La Niña pattern (cluster pattern 1). In recent two decades, it strongly develops towards a positive E index phase with a larger departure from C index, corresponding to the extreme warm events in clusters 2 and 9. It seems that few extreme warm events resemble the El Niño Modoki pattern with a large amplitude of PC3. But the most extreme warm events of El Niño are featured by the canonical El Niño (cluster pattern 9) or the basin-wide warm patterns (cluster pattern 2).

In the early stage of 1950–1969, the background mode provided a favourable initial disturbance for the warm event, so the observed warm events always originated and developed from cluster pattern 3 in the EP. In most cases, the cold events often originated from the cold SSTA in the eastern tropical Pacific (cluster pattern 1). Recently, pattern 3 is replaced by pattern 8 with a cold tongue SSTA mode in the eastern tropical Pacific, but the observed extreme cold events often started in the CP (cluster pattern 7) instead of the EP, which may be accounted for the asymmetrical responses of the cold and warm events. The extreme La Niña events tends to originate from the CP, which is suggested to be highly correlated with the Maritime region-CP temperature gradient through Bjerknes positive feedback (Cai *et al.*, 2015a).

The recently observed extreme warm events often started from cluster pattern 2 or 10 with a strong warm subtropical SSTA, showing especially that pattern 10 is similar to the so-called PMM (Chiang and Vimont, 2004) and implying the important role of the subtropical forcing in the CP El Niño dynamics (Paek *et al.*, 2017). Here it is hypothesized that the increased frequency and amplitude of the extreme warm events of SSTA may be caused by the cooperative impacts of EP, CP dynamics and the subtropical atmosphere forcing. From our result in Figure 6, the extreme warm and extreme cold events both increase in frequency and amplitude in recent decades. As indicated by Cai *et al.* (2015b), an extreme La Niña event tends to evolve into following a strong El Niño event, which is suggested to be a possible reason for the shift of the recent stage in both C index and E index.

To confirm the change of the relationship between the two intrinsic modes under global warming, the 10-year running correlation is applied to PC1 and PC3 (Figure S3). The significantly positive correlation between

PC1 and PC3 can be detected in recent decades. This implies that the distinction of two regimes of SSTA defined by Takahashi *et al.* (2011) becomes more obvious under global warming. In addition, the maximum slope difference between the period of 1950–1969 and 1997–2016 appeared in boreal spring and winter (as shown in Figure S4), implying that the regimes of the tropical Pacific SSTA become most distinct in these seasons.

6 | SUMMARY AND DISCUSSION

Based on the three leading EOF modes of the SSTA variability in the tropical Pacific during 1950–2016, the ENSO-related SSTA can be classified into two SSTA intrinsic modes (EOF1 and EOF3) and a background mode (EOF2). The two intrinsic modes are related to the ENSO regimes, E index and C index regimes, which becoming more distinct, especially in boreal spring and winter under recent global warming. While the background mode with a slowly increasing east–west SSTA gradient is very likely associated with recent global warming. In the framework of the combination of these three modes, 10 cluster patterns are identified and analysed. Results suggested that the basin-wide warm events and CP cold events occurred more frequently under global warming during 1950–2016.

The observed background mode changed from negative to positive phases around the middle 1980s, showing an opposite SSTA in the early and recent decades. Before the middle 1980s, the cooling SSTA revealed by cluster pattern 3 covered nearly the whole tropical Pacific, with conspicuous exceptions in the warm tongue in the EP. In recent decades, however, it was replaced by a cooling tongue pattern in this region. According to the asymmetry of ENSO (Cai *et al.*, 2015b), El Niño and La Niña events prefer to develop in the eastern equatorial Pacific in the earlier stage of global warming. However, in recent decades, more extreme La Niña events originate from the CP as the enhanced background mode of SSTA. Our results also suggested that the increasing frequency and amplitudes of both the El Niño and La Niña events imply more basin-wide warming and extreme El Niño events as well as more extreme central La Niña events. In addition, the results also showed that the distinction between the regular and extreme warm SSTA regimes have become more noticeable under global warming. The change of the SSTA patterns diversity is attributed to both the background mode with enhanced east–west SST gradient and the change in composition of intrinsic modes. From our results, the asymmetric response to the background mode is hypothesized to be the source of enhanced distinct SSTA regimes resulting in the change of the ENSO diversity.

Recently, Xu *et al.* (2017) investigated the future projections of EP and CP types warm ENSO events using historical and RCP8.5 (representative concentration pathway) runs in the phase of the Coupled Model Intercomparison Project (CMIP5). In their study, the two intrinsic modes were used to describe EP and CP modes so they pointed out that the models have the same frequencies of the two modes in the present and future climate, but robust changes in the tropical precipitation connected with SSTA patterns can be found. Many previous studies focused on the two intrinsic modes respectively as EP and CP modes. Clearly, the two intrinsic modes of SSTA are stable under global warming. The change of the ENSO diversity is mainly attributed to the changing composition of the intrinsic modes rather than the change of modes themselves. Results of this study suggest that the change in composition of the two SSTA intrinsic modes should be paid more attention, instead of either of them, while studying the linkage between global warming and SSTA patterns.

ACKNOWLEDGEMENT

This research was supported by the Discipline Layout Project for Basic Research of Shenzhen Science and Technology Innovation Committee (Grant No. JCYJ20170810103011913) and the National Natural Science Foundation of China (Grant No. 41790473).

ORCID

Jing Li  <https://orcid.org/0000-0002-0395-2571>

Linhao Zhong  <https://orcid.org/0000-0003-2833-1808>

REFERENCES

- Ashok, K., Behera, S.K., Rao, S.A., Weng, H. and Yamagata, T. (2007) El Niño Modoki and its possible teleconnection. *Journal of Geophysical Research*, 112(C11), C11007. <https://doi.org/10.1029/2006JC003798>.
- Ashok, K., Sabin, T.P., Swapna, P. and Murtugudde, R.G. (2012) Is a global warming signature emerging in the tropical Pacific? *Geophysical Research Letters*, 39(2), L02701. <https://doi.org/10.1029/2011GL050232>.
- Brohan, P., Kennedy, J.J., Harris, I., Tett, S.F.B. and Jones, P.D. (2006) Uncertainty estimates in regional and global observed temperature changes: a new data set from 1850. *Journal of Geophysical Research Atmospheres*, (D12), 111.
- Cai, W., Borlace, S., Lengaigne, M., Van, R.P., Collins, M., Vecchi, G., Timmermann, A., Santoso, A., Mcphaden, M.J., Wu, L., England, M.H., Wang, G., Guilyardi, E. and Jin, F. (2014) Increasing frequency of extreme El Niño events due to greenhouse warming. *Nature Climate Change*, 5(1), 1–6. <https://doi.org/10.1038/nclimate2100>.
- Cai, W., Santoso, A., Wang, G., Yeh, S.-W.W., An, S.-I., Cobb, K.M., Collins, M., Guilyardi, E., Jin, F.-F., Kug, J.-S.S., Lengaigne, M., Mcphaden, M.J., Takahashi, K., Timmermann, A., Vecchi, G., Watanabe, M. and Wu, L. (2015a) ENSO and greenhouse warming. *Nature Climate Change*, 5(9), 849–859. <https://doi.org/10.1038/nclimate2743>.
- Cai, W., Wang, G., Santoso, A., Mcphaden, M.J., Wu, L., Jin, F.F., Timmermann, A., Collins, M., Vecchi, G., Lengaigne, M., England, M.H., Dommenges, D., Takahashi, K. and Guilyardi, E. (2015b) Increased frequency of extreme La Niña events under greenhouse warming. *Nature Climate Change*, 5(2), 132–137. <https://doi.org/10.1038/nclimate2492>.
- Cane, M.A., Clement, A.C., Kaplan, A., Kushnir, Y., Pozdnyakov, D., Seager, R., Zebiak, S.E. and Murtugudde, R. (1997) Twentieth-century sea surface temperature trends. *Science*, 275(5302), 957–960. <https://doi.org/10.1126/science.275.5302.957>.
- Capotondi, A., Wittenberg, A.T., Newman, M., Di Lorenzo, E., Yu, J.-Y., Braconnot, P., Cole, J., Dewitte, B., Giese, B., Guilyardi, E., Jin, F.-F., Karneuskas, K., Kirtman, B., Lee, T., Schneider, N., Xue, Y. and Yeh, S.-W. (2015) Understanding ENSO Diversity. *Bulletin of the American Meteorological Society*, 96(6), 921–938. <https://doi.org/10.1175/BAMS-D-13-00117.1>.
- Chiang, J.C.H. and Vimont, D.J. (2004) Analogous Pacific and Atlantic meridional modes of tropical atmosphere – ocean variability. *Journal of Climate*, 17, 4143–4158. <https://doi.org/10.1175/JCLI4953.1>.
- Ding, S., Chen, W., Graf, H.F., Guo, Y. and Nath, D. (2018) Distinct winter patterns of tropical Pacific convection anomaly and the associated extratropical wave trains in the Northern Hemisphere. *Climate Dynamics*, 51(5–6), 2003–2022. <https://doi.org/10.1007/s00382-017-3995-0>.
- Fedorov, A.V. and Philander, S.G. (2000) Is El Niño changing? *Science*, 288(5473), 1997–2002. <https://doi.org/10.1126/science.288.5473.1997>.
- Hoerling, M.P., Kumar, A. and Min, Z. (1997) El Niño, La Niña, and the nonlinearity of their teleconnections. *Journal of Climate*, 10(8), 1769–1786.
- Huang, B., Banzon, V.F., Freeman, E., Lawrimore, J., Liu, W., Peterson, T.C., Smith, T.M., Thorne, P.W., Woodruff, S.D. and Zhang, H.-M. (2015) Extended reconstructed sea surface temperature version 4 (ERSST.v4). Part I: upgrades and intercomparisons. *Journal of Climate*, 28(3), 911–930. <https://doi.org/10.1175/JCLI-D-14-00006.1>.
- Ishii, M., Shouji, A., Sugimoto, S. and Matsumoto, T. (2005) Objective analyses of sea-surface temperature and marine meteorological variables for the 20th century using ICOADS and the Kobe collection. *International Journal of Climatology*, 25(7), 865–879.
- Jiang, N., Qian, W. and Leung, J.C.H. (2016) The global monsoon division combining the k-means clustering method and low-level cross-equatorial flow. *Climate Dynamics*, 47(7–8), 2345–2359. <https://doi.org/10.1007/s00382-015-2967-5>.
- Johnson, N.C. (2013) How many ENSO flavors can we distinguish. *Journal of Climate*, 26(13), 4816–4827. <https://doi.org/10.1175/JCLI-D-12-00649.1>.
- Kaufman, L. and Rousseeuw, P.J. (1990) Finding groups in data: an introduction to cluster analysis. *Biometrics*. New York: John Wiley & Sons. <https://doi.org/10.2307/2532178>.
- L’Heureux, M.L., Collins, D.C. and Hu, Z.-Z. (2013) Linear trends in sea surface temperature of the tropical Pacific Ocean and implications for the El Niño-southern oscillation. *Climate Dynamics*, 40(5–6), 1223–1236. <https://doi.org/10.1007/s00382-012-1331-2>.

- Leloup, J.A., Lachkar, Z., Boulanger, J.P. and Thiria, S. (2007) Detecting decadal changes in ENSO using neural networks. *Climatic Dynamics*, 28(2–3), 147–162. <https://doi.org/10.1007/s00382-006-0173-1>.
- Ogbuabor, G. and Ugwoke, F.N. (2018) Clustering algorithm for a healthcare dataset using Silhouette score value. *International Journal of Computer Science and Information Technology*, 10(2), 27–37. <https://doi.org/10.5121/ijcsit.2018.10203>.
- Paek, H., Yu, J.-Y. and Qian, C. (2017) Why were the 2015/2016 and 1997/1998 extreme El Niños different? *Geophysical Research Letters*, 44(4), 1848–1856. <https://doi.org/10.1002/2016GL071515>.
- Power, S., Delage, F., Chung, C., Kociuba, G. and Keay, K. (2013) Robust twenty-first-century projections of El Niño and related precipitation variability. *Nature*, 502(7472), 541–545. <https://doi.org/10.1038/nature12580>.
- Rayner, A.N., Rayner, N.A., Parker, D.E., Horton, E.B., Folland, C.K., Alexander, L.V. and Rowell, D.P. (2003) Global analyses of sea surface temperature, sea ice, and night marine air temperature since the late nineteenth century. *Journal of Geophysical Research*, 108(D14), 4407. <https://doi.org/10.1029/2002JD002670>.
- Su, J., Lian, T., Zhang, R. and Chen, D. (2018) Monitoring the pendulum between El Niño and La Niña events. *Environmental Research Letters*, 13(7), 074001. <https://doi.org/10.1088/1748-9326/aac53f>.
- Takahashi, K., Montecinos, A., Goubanova, K. and Dewitte, B. (2011) ENSO regimes: reinterpreting the canonical and Modoki El Niño. *Geophysical Research Letters*, 38(10), L10707. <https://doi.org/10.1029/2011GL047364>.
- Wittenberg, A.T. (2009) Are historical records sufficient to constrain ENSO simulations? *Geophysical Research Letters*, 36, L12702. <https://doi.org/10.1029/2009GL038710>.
- Xu, K., Tam, C.Y., Zhu, C., Liu, B. and Wang, W. (2017) CMIP5 projections of two types of El Niño and their related tropical precipitation in the twenty-first century. *Journal of Climate*, 30(3), 849–864. <https://doi.org/10.1175/JCLI-D-16-0413.1>.
- Yeh, S., Kug, J., Dewitte, B., Kwon, M., Kirtman, B.P. and Jin, F. (2009) El Niño in a changing climate. *Nature*, 461(7263), 511–514. <https://doi.org/10.1038/nature08316>.
- Yeh, S.W., Kug, J.S. and Il, A.S. (2014) Recent progress on two types of El Niño: observations, dynamics, and future changes. *Asia-Pacific Journal of Atmospheric Sciences*, 50(1), 69–81. <https://doi.org/10.1007/s13143-014-0028-3>.
- Zebiak, S. and Cane, M. (1987) A model El Niño-southern oscillation. *Monthly Weather Review*, 115(1985), 2262–2278.
- Zhang, W., Li, J., Zhao, X. and Xia, Z. (2010) Sea surface temperature cooling mode in the Pacific cold tongue. *Journal of Geophysical Research: Oceans*, 115(12), C12042. <https://doi.org/10.1029/2010JC006501>.

SUPPORTING INFORMATION

Additional supporting information may be found online in the Supporting Information section at the end of this article.

How to cite this article: Li J, Mu L, Zhong L. Distinct tropical Pacific sea surface temperature anomaly regimes enhanced under recent global warming. *Int J Climatol*. 2021;41:970–979. <https://doi.org/10.1002/joc.6712>